

SEISMIC PERFORMANCE OF ULTRA-HIGH-STRENGTH CONCRETE COLUMNS USING HIGH STRENGTH LONGITUDINAL STEEL BARS

Hassane OUSALEM^{*1}, Hiroto TAKATSU^{*2}, Yuji ISHIKAWA^{*3} and Hideki KIMURA^{*4}

ABSTRACT

This paper discusses the test results of three Steel-Fiber High-Strength-Concrete columns subjected axially to constant or varying axial loads and laterally to increasing reverse cycles. Strength, deformation, crack development and other features are presented. The investigated parameter is the strength of longitudinal reinforcement. While two types of high strength steel bars are used for longitudinal bars (SD980 of $\sigma_y=980\text{MPa}$ and SD685 of $\sigma_y=685\text{MPa}$), concrete strength (171MPa) and transverse reinforcement are similar for all specimens. The advantage of using very high strength steel bars is discussed.

Keywords: high-strength steel, steel fiber, ultra-high-strength-concrete, varying axial load

1. INTRODUCTION

The crucial need of high strength materials to achieve high structural performances has been the consequence of the ever-increasing need for vertical expansion of metropolitan cities owing to the over-inflated prices of land and/or to the increase in the hazard of the region and/or to the evaluated level of induced loads due to different causes.

The historical development and technical characteristics of high strength materials (HSM), particularly those used in reinforced concrete (RC), were well illustrated by Okamura et al. [1], Schmidt and Fehling [2] and Mertol et al. [3]. The recorded slow use of HSM in RC structures has mainly been due to the limitations included in the regulations. Actually, such limitations reflected the lack of research data and confidence rather than the inability of the materials to perform their intended function. However, since some recent catastrophic events, for instance seismic ones, high seismic structural performance has been required and become a great social demand where the life-cycle cost has to be considered for any engineering solution.

To reach that purpose, analytical and experimental works investigating the behavior of high strength concrete (HSC) columns have been carried out. Konstantinidis [4] made an analytical

study on the seismic response of 22 15-story buildings assuming different element properties. The author concluded that the benefit of utilizing high strength/yield steel (HSS/HYS) as transverse reinforcement was not fully exploited for the beams, while utilizing HYS as longitudinal reinforcement in the columns kept the response essentially elastic. Sun and Fukuhara [5] carried out tests on four RC frames simulating the behavior of HSC elements at the lower story of high-rise buildings. Their work investigated tube confinement as an alternative to the conventional one in order to overcome steel congestion problems and concrete splitting and reached good conclusions but the study omitted the cost side. To achieve similar objectives, Takatsu et al. [6] used HSS (SD685 for main bars and SPBD1275/1420 for stirrups) in their 10 tested columns and investigated successfully the influence of steel fiber (SF) volumetric ratio on columns' behavior. An ultra high concrete strength of 150MPa was achieved and columns proved to be ductile where early spalling of cover concrete was delayed, surface crack width reduced and lateral capacity increased when fiber volume ratio increased.

The work presented herein aims to improve the behavior of SF HSC columns by increasing considerably the concrete strength and investigates the applicability of very HSS (SD980) longitudinal reinforcement.

*1 Researcher, Takenaka Research and Development Institute, Dr., JCI Member

*2 Researcher, Takenaka Research and Development Institute, M.E., JCI Member

*3 Chief Researcher, Takenaka Research and Development Institute, Dr.E., JCI Member

*4 Chief Researcher, Takenaka Research and Development Institute, Dr.E., JCI Member

2. TEST PROGRAM

2.1 Specimens

Three 1/4-scaled column specimens, designed according to Japanese regulations and considered representative of those occurring in the first story of tall buildings, were built and tested. All columns had the same cross section of 280mm x 280mm (b x D), the same length of 1120mm (L), the same shear span ratio of 2, the same transverse and longitudinal reinforcement ratios, respectively, 1.22% (ρ_w , 3- ϕ 7.1/35mm) and 2.92% (ρ_g , 8-D19) and the same concrete with a steel fiber volumetric ratio V_f of 1%. The difference between specimens was in the type of main bars and the axial loading. The characteristics of the specimens are shown in Table 1 and a scheme is depicted in Fig. 1.

2.2 Materials

(1) Reinforcing materials

High tensile steel fibers with an aspect ratio of 79 (30mm long and 0.38mm diameter) and hooked ends were mixed to concrete. Two types of D19-steel bars were used as longitudinal reinforcement (SD685 and SD980). Another type of ϕ 7.1-steel was used as transverse reinforcement (SPBD1275/1420). The properties of tested steel bars are shown in Table 2 and Fig. 2.

Table 1 Characteristics of specimens

Specimen	Main bar type	Axial Loading
Unit 700	SD685	Varying
Unit 701	SD980	Varying
Unit 702	SD980	Constant

Table 2 Characteristics of reinforcements

Type	Elastic Modulus	Tensile strength	
	(kN/mm ²)	σ_v (N/mm ²)	σ_u (N/mm ²)
D19 (SD685)	189	740	1000
D19 (SD980)	188	1201*	1287
ϕ 7.1(SPBD1275/1420)	193	1361*	1430

*0.2% off-set yield stress

Table 3 Applied axial load ratios

Specimen	Initial load ratio	Minimum load ratio	Maximum load ratio
	η_0	η_t	η_c
Unit 700	0.2	-0.71	0.6
Unit 701	0.2	-0.71	0.6
Unit 702	0.3	-	0.3

$\eta_0 = N_0 / (bDF_c)$, $\eta_c = N_c / (bDF_c)$, $\eta_t = N_t / (\rho_g bD\sigma_y)$

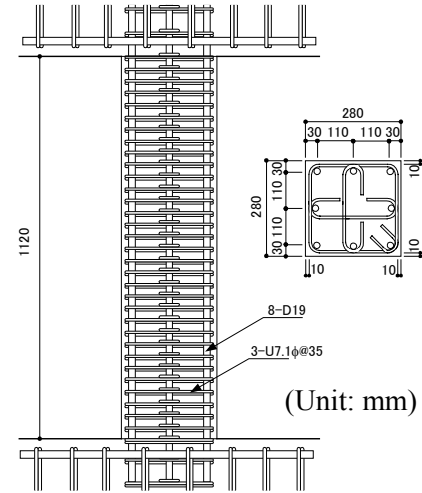


Fig.1 Geometric details of test specimens

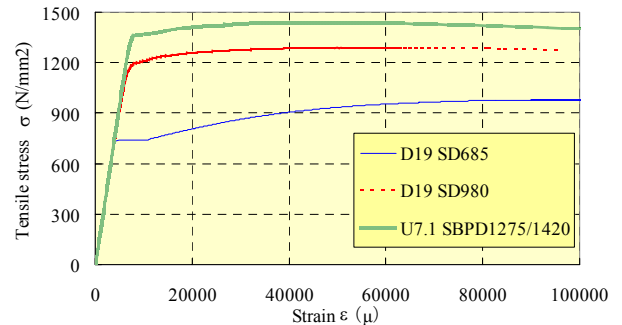


Fig.2 Characteristics of reinforcements

(2) Concrete

Using 13mm maximum size coarse aggregates, 15% average of water/cement ratio and 1% volumetric ratio of steel fibers, resulted in the average density of 2.51t/m³. The average concrete strength F_c and Young's modulus E_c , obtained from cylinder tests after a 72-hour thermal curing, were, respectively, 171MPa and 4.52×10^4 MPa.

2.3 Loading Method

All specimens were tested in a vertical position using a pantograph with a vertical jack on the top of specimens for compression load, two vertical side-jacks for tension load and one horizontal jack for lateral load. Laterally, specimens were subjected to an anti-symmetric double curvature bending where the loading path was controlled by displacement. Reversed cycles with increasing lateral drift angle amplitude R from 0.1% till 5% were applied in one direction. The axial load N , when varied, was proportional to the lateral shear force Q , where the initial, tension and compression ratios are illustrated in Table 3 and Fig. 3. The maximum compression load was equal for the Unit-700 and Unit-701 while the maximum tension force was higher in Unit-701.

3. OBSERVED BEHAVIOR AND ELEMENT RESPONSE

Tested specimens experienced various stages till the end of loading. Degradation in strength was due to concrete damage and a probable buckling although no clear sign of main bars buckling was noticed. The advantage of using SF appeared clearly from the limited and narrow cracks on the whole surface till $R = -0.5\%$ and on the column's central face zone till $R = -1.5\%$. The advantage of using HSS bars appeared slightly on the positive loading (compression) side but appeared on the negative loading (tension) side and also through the delay of some stages.

3.1 Cracks development and damage

For specimens under varying axial load, similar crack patterns were generally observed although some delay for the specimen with very HSS (SD980) bars when cracks spread out beyond $R = -0.33\%$. Tension cracks developed mainly when loading direction was on the tension side while crushing appeared when loading direction was on compression side. Unit-700 (specimen with SD685) experienced bending cracks, bending shear cracks, crushing of concrete and yielding of compression steel bars at column ends section, respectively, at $R = -0.10\%$, -0.20% , 0.33% and 0.50% . Yielding of tension steel bars at column ends section occurred at $R = 2.60\%$. Yielding of steel bars extended from column ends section till a distance $D/2$ for compression and tension bars and till a distance D for only compression bars. Damage concentrated at the compression corners since $R = 0.75\%$ and discontinuous splitting cracks formed along the main-bars location after $R = 1.00\%$. Unit-701 (specimen with SD980) experienced bending cracks, bending shear cracks and crushing of concrete, respectively, at $R = -0.11\%$, -0.20% and 0.33% . Due to probable defections in strain gauges caused by thermal curing, yielding was recorded only on one central bar at $R = -3.00\%$ while all other main bars seemed remain elastic. Damage concentrated at the compression corners since $R = 0.75\%$ and splitting cracks did not form along the main-bars location. On both specimens, as it can be seen later on the force response curve, it seemed that rupture of some main bars occurred somewhere but unfortunately was not visible when checked at the end of loading.

For the specimen under constant axial load (Unit-702, specimen with SD980), compared to the specimens under varying axial load, the crack pattern was different and cracks started at $R =$

0.20% with small vertical cracks at corners, followed by bending cracks, bending-shear cracks, crushing of concrete and yielding of compression steel bars at column ends section, respectively, at $R = 0.33\%$, 0.60% , 0.75% and 2.00% . Damage concentrated mainly at the corners of the specimen ends region and splitting cracks spread along the main-bars location since $R = 1.00\%$. Fig. 4 shows specimens' condition at different drift angles.

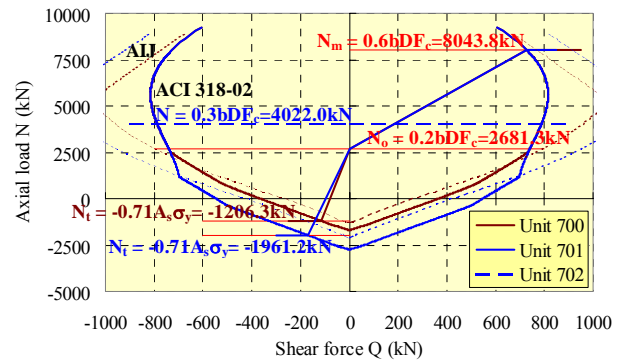


Fig.3 Q-N interaction diagram and axial load

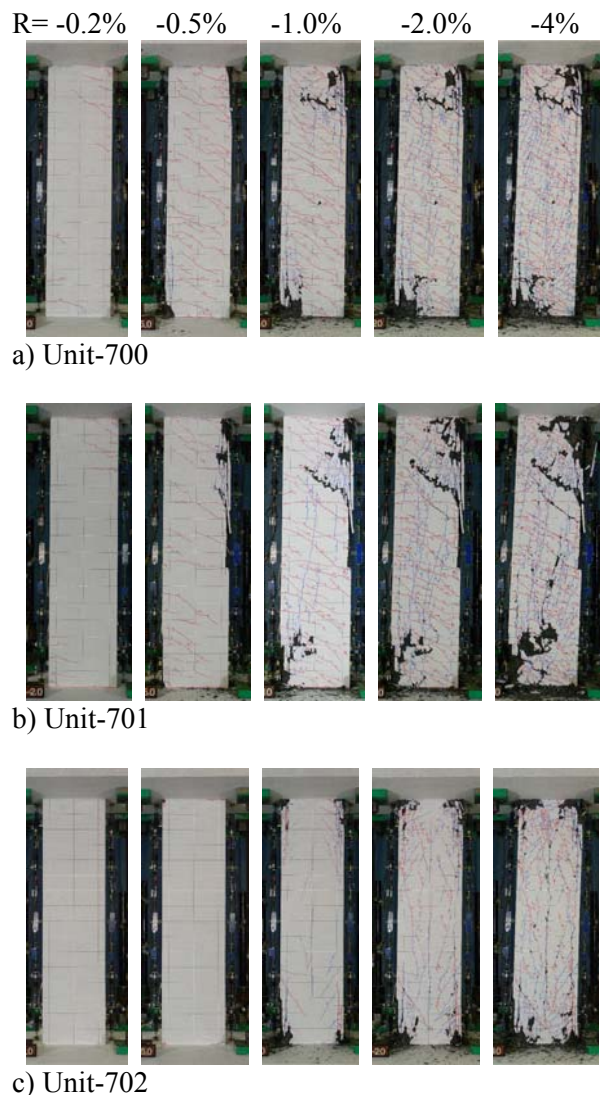


Fig.4 Cracks evolution and damage

Crack-width could be recorded after $R=0.2\%$ and 1.0% , respectively, for the specimens under varying axial load and the specimen under constant axial load. Maximum widths were recorded at columns' end regions, particularly those coming from bending. However, records could not be kept continuous at different locations due to crushing, splitting and damage of concrete. In Unit-700, cracks far from crushing places reached a maximum width of 0.1mm while those inside the damaged region went beyond 1.5mm before splitting of concrete. In Unit-701, cracks far from crushing places had a limited width (0.06mm) while those inside reached a maximum width of 0.35mm at $R=2.0\%$. In Unit-702, crack-width was also limited and reached 0.03mm for bending cracks and 0.45mm for shear cracks in the columns' end region at $R=-5.0\%$. Far from the columns end region, vertical cracks reached a width of 0.25mm at columns' mid-height.

3.2 Elements strength and deformability

(1) Shear force response and strength degradation

Response of the specimens to the applied loads varied according to the loading direction.

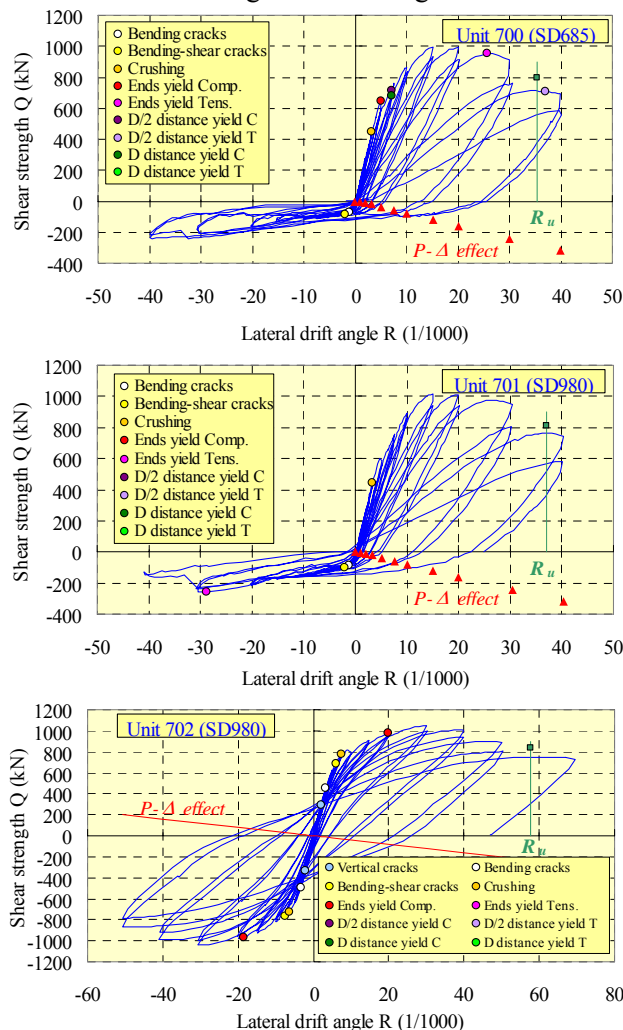


Fig.5 Shear force response

Table 4 Performance of specimens

Spec.	Q_{\max} (kN)	R_{\max} (%)	R_u (%)	Q_{ACI} (kN)	Q_{AIJ} (kN)
Unit 700	995.9 (-241.2)	1.51 (-3.25)	3.53	725.8 (-113.5)	767.7 (-13.6)
Unit 701	1015.0 (-260.4)	1.50 (-3.05)	3.70	725.8 (-171.4)	915.3 (-21.0)
Unit 702	1045.9	3.02	5.76	787.6	1117.1

(-x.x): value on tension-negative loading side

R_u : ultimate drift angle at 20% strength decay

Test strength values were higher between 30 and 40%, and between 10 and 30%, respectively, than those given by ACI and AIJ. Table 4 presents the main results and Fig. 5 shows the global behavior of each specimen.

When lateral loading direction was on the positive side (compression side for varying axial loading), Unit-701 and Unit-702 showed similar strengths slightly higher than Unit-700. Unit-702 was the most ductile where shear strength degradation after peak (inclination of the envelope curve) was the lowest. Compared to Unit-700, Unit-701 showed lower shear strength degradation and residual displacements at unloading stages are also slightly lower.

When lateral loading direction was on the negative side (tension side for varying axial loading), Unit-701 showed slightly higher stiffness and reached higher strength at lower lateral drift but was less ductile than Unit-700 due to high applied tension load (30% higher in Unit-701 than in Unit-700). The test on Unit-701 was interrupted for safety reasons where the specimen showed a sudden decrease in strength on the tension side (a rupture of main bars that could neither be checked visually nor on strain data). Due to the limited crack-width in Unit-701, compared to Unit-700, the specimen had slightly higher stiffness during the unloading and reloading stage.

Unit-702, under constant axial load, had a smooth and symmetric response on both loading sides. The axial loading level could be considered favorable and less damaging than the loading level applied in Unit-701. Higher constant axial load ratio would probably induce a similar degradation response as in Unit-701.

Fig. 6 compares test results to some previously tested similar columns where it shows the advantage of using higher concrete strength combined to higher steel strength.

(2) Strains of reinforcements

The recorded strains of reinforcement at different locations confirmed the lower values in

HSS. Generally, strains of the main bars in specimens under varying axial load were lower for extreme and center bars at column ends when SD980-HSS was used as shown in Fig. 7. Also, when load conditions were comparable (positive lateral loading side), compression or tension strains of HSS in the specimen under constant axial load (Unit-702 with lower axial load) were higher than those in the specimen under varying axial load (Unit-701 with higher axial load) due to the difference level in the applied axial force and the combined resulting moment. Table 5 illustrates the maximum level recorded at different locations and heights.

As to the transverse reinforcement, the strains varied along columns heights at different loading stages. Strains in the stirrups were higher than strains in the individual legs. Strains in steel-elements parallel to the lateral loading direction were higher than strains in steel-element perpendicular to the loading direction.

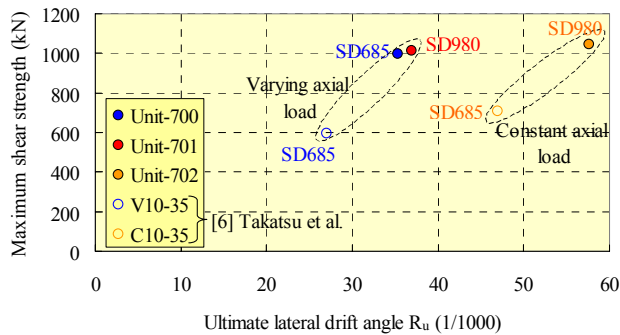


Fig.6 Comparison of some test results

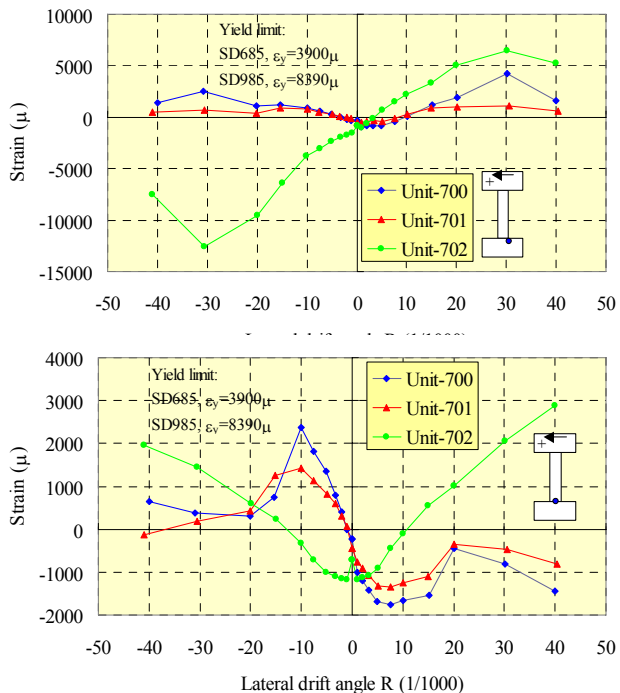


Fig.7 Strain evolution in main bars

Table 5 Main bars max. strain ratio ($\epsilon_{max}/\epsilon_y$)

Spec.	Stress	Lower End*	D/2**	D**	Upper End*
Unit-700	C	2.50	1.30	2.00	2.50
	T	1.30	1.80	0.90	1.30
Unit-701	C	0.25	0.25	0.25	1.20
	T	0.25	0.25	0.25	0.50
Unit-702	C	1.30	0.75	0.50	0.25
	T	1.30	0.75	0.50	0.25

Note: C=Compression; T=Tension; D=Column section height; *=Column end; **=Distance from the bottom

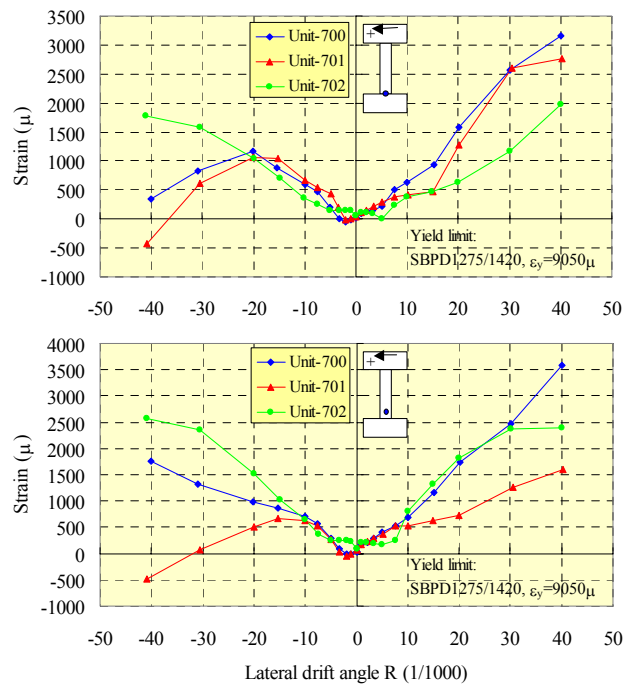


Fig.8 Strain evolution in transverse steel

In specimens subjected to varying axial load recorded strains were similar before $R=\pm 1.0\%$ but lower for the specimen with SD980 bars beyond that drift angle, particularly inside the hinge zone. The recorded maximum strain in both specimens was less than $0.5\epsilon_y$. In the specimen subjected to constant axial load, when loading conditions were comparable, strains were similar to those in Unit-701 particularly in the hinge zone and lower elsewhere. The recorded maximum strain was less than $0.33\epsilon_y$. Fig. 8 illustrates the strain evolution recorded in the stirrups at the column end and at the mid-hinge zone.

(3) Deformability and energy dissipation

The tested specimens reached large lateral deformability, allowing larger ductility when low constant axial-compression load was applied. Shear displacement decreased along loading due to flexural damage at columns' ends. Average shear displacement at $R=1.0\%$ (-1.0%) accounted for almost 20% (30%) of the total displacement

for Unit-700 and 20% (20%) for Unit-701 and 20% (20%) for Unit-702.

Axially, the deformation was the highest (column shortening) at neutral position ($R=0.0\%$) and the lowest at maximum drift angles when constant axial load was applied. For the specimens under varying axial load, the axial deformation was lower (shortening or elongation) in Unit-701 than in Unit-700 at neutral position but similar for both specimens at maximum drift angles, as shown in Fig. 9.

Although the slightly low residual drift recorded on Unit-701 compared to Unit-700, the specimens showed similar ability to dissipate energy when the axial force was compression with slightly higher dissipation level in the specimen with constant axial load beyond $R=0.5\%$, as shown in Fig. 10 through equivalent damping ratio.

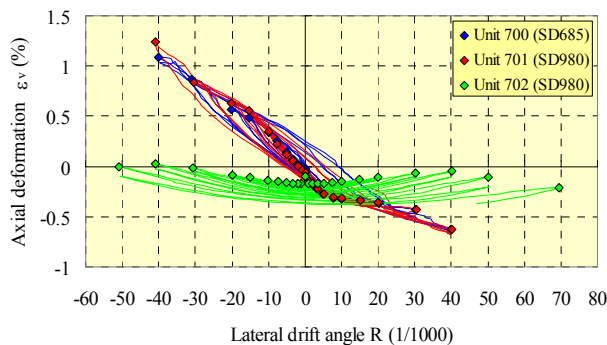


Fig.9 Axial deformation

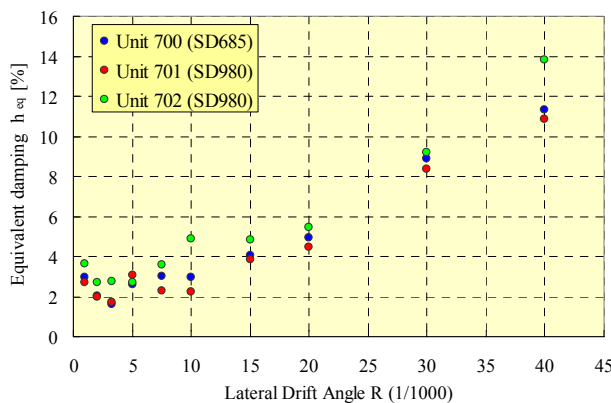


Fig.10 Equivalent damping

5. CONCLUSIONS

- (1) No sign of buckling on all steel bar types
- (2) Benefit of using SF appears in the limited and narrow crack-widths before $R= -0.5\%$, particularly when SD980 steel is used
- (3) Use of SD980 steel delays cracks evolution outside hinge zone beyond $R= -0.33\%$
- (4) Damage concentration is similar for both steel types till $R= 0.75\%$ but beyond that

- limit it appears more abrupt for SD980 steel.
- (5) Use of SD980 steel induces slightly higher column stiffness than SD685 steel and results in slightly higher strength
- (6) Use of SD980 steel induces lower column shear strength degradation, higher ductility (larger ultimate drift angle R_u) and smaller residual deformation than SD685 steel
- (7) Use of SD980 steel lowers column shear deformation in the range $R= \pm 1\%$ than the SD685 steel, particularly on tension side.
- (8) Use of SD980 steel reduces strains of stirrups inside hinge region beyond $R= 1.0\%$
- (9) Use of SD980 steel doesn't affect significantly the energy absorption compared to SD685 steel.
- (10) Use of SD980 steel lowers the axial deformation at neutral position but doesn't affect it at large drift angles
- (11) Axial loading type affects the crack development and damage concentration for columns of similar high strength steel type

REFERENCES

- [1] Okamura, H., Maekawa, K. and Mishima T., "Performance Based Design for Self-Compacting Structural High-Strength Concrete," 7th Int. Sym. on the Utilization of HS/HPC, Washington, Editor Henry G. Russel, ACI, SP-228-2, pp. 13-34, June 2005
- [2] Schmidt, M. and Fehling, E., "Ultra-High-Performance Concrete: Research, Development and Application in Europe," 7th Int. Sym. on the Utilization of HS/HPC, SP-228-4, pp. 51-77, June 2005
- [3] Mertol, H.C. et al., "Behavior and Design of HSC Members Subjected to Axial Compression and Flexure," 7th Int. Sym. on the Utilization of HS/HPC, P-228-28, pp. 395-419, June 2005
- [4] Konstantinidis, D., "Seismic Response of High-Rise RC Buildings Made of High-Strength Materials," 7th Int. Sym. on the Utilization of HS/HPC, SP-228-39, pp. 595-614, June 2005
- [5] Sun, Y. and Fukuhara, T., "Development of High Seismic Performance Concrete Frames," 7th Int. Sym. on the Utilization of HS/HPC, SP-228-40, pp. 615-632, June 2005
- [6] Takatsu, H. et al., "Experimental Study of Steel Fiber-Reinforced Ultra High-Strength Concrete Columns," Proceedings (CD) of the 2nd Int. Congress, FIB, Naples, ID 8-17, 10pages, June 2006